Photoresponsive Supramolecular Systems: Synthesis and Photophysical and Photochemical Study of Bis-(9,10-anthracenediyl)coronands AAO_nO_n

Damien Marquis, Jean-Pierre Desvergne,* and Henri Bouas-Laurent

Laboratoire de Photochimie Organique, CNRS URA 348, Université Bordeaux I, 33405 Talence Cedex, France

Received July 28, 1995[⊗]

Monocyclic bis-(9,10-anthracenediyl)coronands denoted AAO_nO_n (A = (9,10-anthracenediyl, *n* indicating the number of ethyleneoxy repeating units between two aromatic rings) were designed as photoresponsive systems. Their synthesis is described; their spectroscopic properties were found to be in agreement with the X-ray structures. Special attention was devoted to AAO_5O_5, which gives coronates with Na^+ and K^+. It was observed that one molecule of AAO_5O_5 displays a positive cooperative effect in binding two sodium cations, in contrast with previous reports on bicyclic coronands. Moreover, in acetonitrile, this effect, clear in the ground state (K_{11} = 180 M^{-1}, K_{12} = 240 M^{-1}) was found to be stronger in the excited state (K_{11} = 200 M^{-1}, K_{12} = 500 M^{-1}). With K^+, AAO_5O_5 generates a 1:1 complex ($K \approx 9$ M^{-1} in methanol). Spectroscopic properties were shown to be triggered by cation concentration, specifically the fluorescence emission which undergoes an important intensity and wavelength redistribution in favor of the excimer: the maximum wavelength is shifted from 530 nm (free ligand) to 570 nm (sodium biscoronate), *i.e.*, $\Delta\bar{\nu}$ ca. 1350 cm^{-1} and the excimer intensity is multiplied by ca. 3. The photocyclomerization (intramolecular dimerization of the anthracene nucleus) was demonstrated to be *regiospecifically directed by* Na^+; in methanol, the free receptor exclusively generates the 9,10:1′,4′ photoadduct ($\Phi_R \approx 2 \times 10^{-4}$) whereas the sodium biscoronate leads to the classical 9,10:9′,10′ photoadduct ($\Phi_R \approx 8 \times 10^{-3}$). Finally, a transient kinetic analysis versus temperature allowed the determination of the conformational mobility of the free receptor within the nanosecond range; in the singlet excited state it is best described by the sequence $M_1^* \rightarrow M_2^* \rightarrow E$ where M* stands for the locally excited state and E the excimer state species. At room temperature, in methanol, excimer lifetimes were found to be as follows: free ligand, 23 ns; sodium biscoronate, 165 ns; and potassium monocoronate, 215 ns.

Introduction

Photoresponsive supramolecular systems are of great interest, particularly for their potential application to nanoscale devices for cation detection, photoreversible cation traps, light-directed ionic switches, light energy devices,[1] etc. Among the photoactive subunits, aromatic hydrocarbons are examined for their fluorescent properties and, sometimes, for their photochemical reactivity (cycloaddition, isomerization, oxidation, etc.).[1d-h]

The anthracene nucleus is known to combine efficient dual (monomer/excimer) fluorescence emission properties and the ability to generate several types of photodimers whose geometry depends on electronic and conformational factors.[2] In order to trigger these properties by conformational modifications through cation complexation, *i.e.*, generate new photoresponsive systems,[1c] macrocyclic crown ethers incorporating two 9,10-anthracenediyl subunits (denoted AAO_nO_n for convenience) were designed.

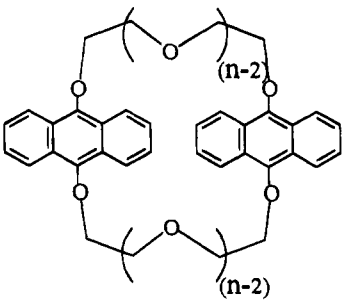

AAO_nO_n
n = 3, 4, 5

A brief description of their preparation was published.[3a] In another preliminary communication, it was shown that the photophysical and photochemical properties of one of these systems AAO_5O_5 can be directed by sodium cations.[3b] Further, it was demonstrated that one AAO_5O_5

[⊗] Abstract published in *Advance ACS Abstracts,* November 1, 1995.

(1) (a) Lehn, J.-M. *Angew. Chem., Int. Ed. Engl.* **1990**, *29*, 1304–1319. (b) *Fiber Optic Chemical Sensors and Biosensors*; Wolfbeis, O. S., Ed.; CRC Press: Boca Raton, FL, 1991; Vols. I and II. (c) Murata, K.; Aoki, M.; Suzuki, T.; Harada, T.; Kawabata, H.; Komori, T.; Ohseto, F.; Ueda, K.; Shinkai, S. *J. Am. Chem. Soc.* **1994**, *116*, 6664–6676. (d) Shinkai, S. In *Molecular Models of Photoresponsiveness*; Montagnoli, G., Erlanger, B. F., Eds.; Plenum: New York, 1983. (e) Shinkai, S.; Manabe, O. *Top. Curr. Chem.* **1984**, *121*, 67–103. (f) Balzani, V. *Supramolecular Photochemistry*; D. Reidel: Dordrecht, 1987. (g) Lehn, J.-M. In *Frontiers in Supramolecular Organic Chemistry and Photochemistry*; Schneider, H. J., Dürr, H., Eds.; VCH: Veinheim, 1991; pp 1–28. (h) Amouyal, E.; Bouas-Laurent, H.; Desvergne, J.-P.; Lapouyade, R.; Valeur, B. *l'Actualité Chimique* (*Suppl. 7*) Dec. **1994**, 182–207. (i) Bissel, R. A.; De Silva, A. P.; Gunaratne, H. N. Q.; Lynch, P. L. M.; Maguire, G. E. M.; Sandanayake, K. R. A. *Chem. Soc. Rev.* **1992**, 187–195. (j) *Fluorescent Chemosensors for Ion and Molecule Recognition*; Czarnik, A. W., Ed.; ACS Symposium Series No. 538; American Chemical Society: Washington, DC, 1992.

(2) (a) Bouas-Laurent, H.; Castellan, A.; Desvergne, J.-P. *Pure Appl. Chem.* **1980**, *52*, 390–397. (b) Desvergne, J.-P.; Fages, F.; Bouas-Laurent, H.; Marsau, P. *Pure Appl. Chem.* **1992**, *52*, 1231–1238. (c) Bouas-Laurent, H.; Desvergne, J.-P. In *Photochromism, Molecules and Systems*; Dürr, H., Bouas-Laurent, H., Eds.; Elsevier: New York, 1990; pp 539–560.

(3) (a) Castellan, A.; Daney, M.; Desvergne, J.-P.; Riffaud, M.-H.; Bouas-Laurent, H. *Tetrahedron Lett.* **1983**, *24*, 5215–5218. (b) Bouas-Laurent, H.; Castellan, A.; Daney, M.; Desvergne, J.-P.; Guinand, G.; Marsau, P.; Riffaud, M.-H. *J. Am. Chem. Soc.* **1986**, *108*, 315–317.

0022-3263/95/1960-7984$09.00/0

Scheme 1. Synthesis of AAO_5O_5 and the Reference Compound R[a]

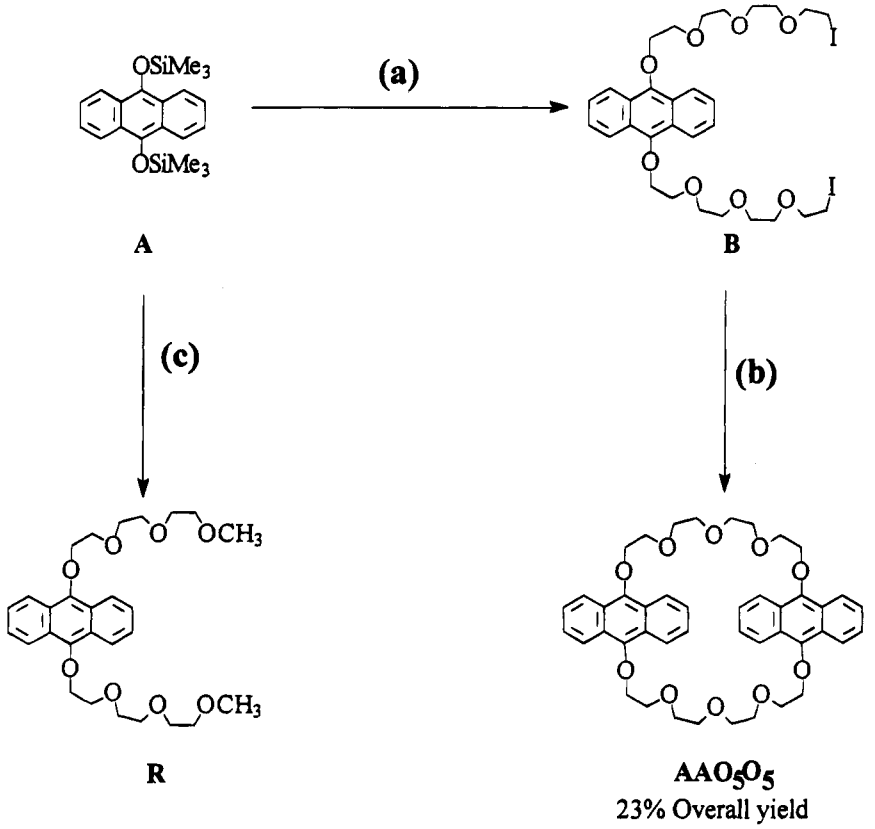

[a] Key: (a) $I(CH_2CH_2O)_3CH_2CH_2I$ (10 mol equiv), K_2CO_3, refluxed acetone, 5 h (72%); (b) K_2CO_3, Cs_2CO_3, refluxed acetone, 4 days (32%); (c) $I(CH_2CH_2O)_3CH_3$, (2.5 mol equiv) K_2CO_3, refluxed acetone, 5 h (18%).

molecule displays a positive cooperativity in binding two metal cations.[4] Here, we report a detailed description of the synthesis, spectroscopic properties, and complexing ability together with the photophysical and photochemical study of AAO_5O_5 in the absence and in the presence of metal cations. Two other coronands AAO_3O_3 and AAO_4O_4 were also investigated, in part, for comparison.

1. Synthesis. Anthracenophane AAO_5O_5 and the reference compound (R) were synthesized from 9,10-bis(silyloxy)anthracene as depicted in Scheme 1.

9,10-Bis(silyloxy)anthracene (A) was obtained from 9,10-anthraquinone by reduction with magnesium powder in the presence of an excess of chlorotrimethylsilane in refluxing THF under argon. Compound A is a masked 9,10-dihydroxyanthracene; the latter can be prepared by reduction of anthraquinone with sodium dithionite[5] but was not selected as intermediate due to its high instability upon exposure to traces of oxygen. After filtration and crystallization in light petroleum ether, the bis(silyloxy) derivative A was isolated in 92% yield as a bright yellow solid in small quantities (3–5 g); the reaction can be scaled up (from 150 g of anthraquinone), but we experienced lower yields, especially at the crystallization stage. Compound A must be stored at low temperature under argon; even then, it slowly generates back anthraquinone after several months. The bis(silyloxy)anthracene (A) was reacted with K_2CO_3 and diiodo-1,11-trioxa-3,6,9-undecane[6] in excess (10-fold) in refluxed acetone to give B in 72% yield. The diiodo compound B and the bis(silyloxy)anthracene A in K_2CO_3/Cs_2CO_3 were mixed under high dilution conditions in refluxed acetone (4 days), giving the bisanthracenyl coronand AAO_5O_5 in 32% yield as a yellow solid. A mixture of K_2CO_3 and Cs_2CO_3 was found to be the more efficient; it is believed that Cs^+ might play a template role during the ring closure stage.[7ab] The diiodo derivative was found to be more convenient (easier separation) than the corresponding ditosylate. The preparation of samples of AAO_5O_5 (0.5–1.0 g) was successfully repeated several times. AAO_3O_3 and AAO_4O_4 were obtained by a one-pot reaction, using similar reactants. The reference compound (R) was prepared in one step in 18% yield (not optimized) following an analogous procedure. The compounds were fully characterized by the usual spectroscopic techniques (see the Experimental Section). The molecular structures of AAO_3O_3[8-10], AAO_4O_4[8-10], and AAO_5O_5[8b] were also established by X-ray diffraction and are fully described elsewhere.[8-10]

2. Electronic Absorption Spectra of AAO_5O_5 (Free Ligand). The absorption spectra of AAO_5O_5, character-

(4) Marquis, D.; Desvergne, J.-P. *Chem. Phys. Lett.* **1994**, *230*, 131–136.

(5) (a) Landucci, L. L.; Ralph, J. *J. Org. Chem.* **1982**, *47*, 3486–3495. (b) Yeung, C. K.; Jasse, B. *Makromol. Chem.* **1984**, *185*, 541–548.

(6) Li, H. M.; Post, B.; Morawetz, H. *Makromol. Chem.* **1972**, *154*, 89–103.

(7) (a) Klieser. B.; Rossa, L.; Vögtle, F. *Kontakte (Darmstadt)* **1984**, *1*, 3–17. (b) Hoss, R.; Vögtle, F. *Angew. Chem., Int. Ed. Engl.* **1994**, *33*, 375–384.

(8) (a) Marsau, P.; Bouas-Laurent, H.; Desvergne, J.-P.; Fages, F.; Lamotte, M.; Hinschberger, J. *Mol. Cryst. Liq. Cryst. Inc. Nonlin. Opt.* **1988**, *156*, 383–392. (b) Guinand, G.; Marsau, P.; Bouas-Laurent, H.; Castellan, A.; Desvergne, J.-P.; Lamotte, M. *Acta Crystallogr.* **1987**, *C 43*, 857–860.

(9) A complete study was not carried out on AAO_3O_3 and AAO_4O_4 as their optical response is not modified in the presence of cations and they were found not to be photoreactive under our experimental conditions.

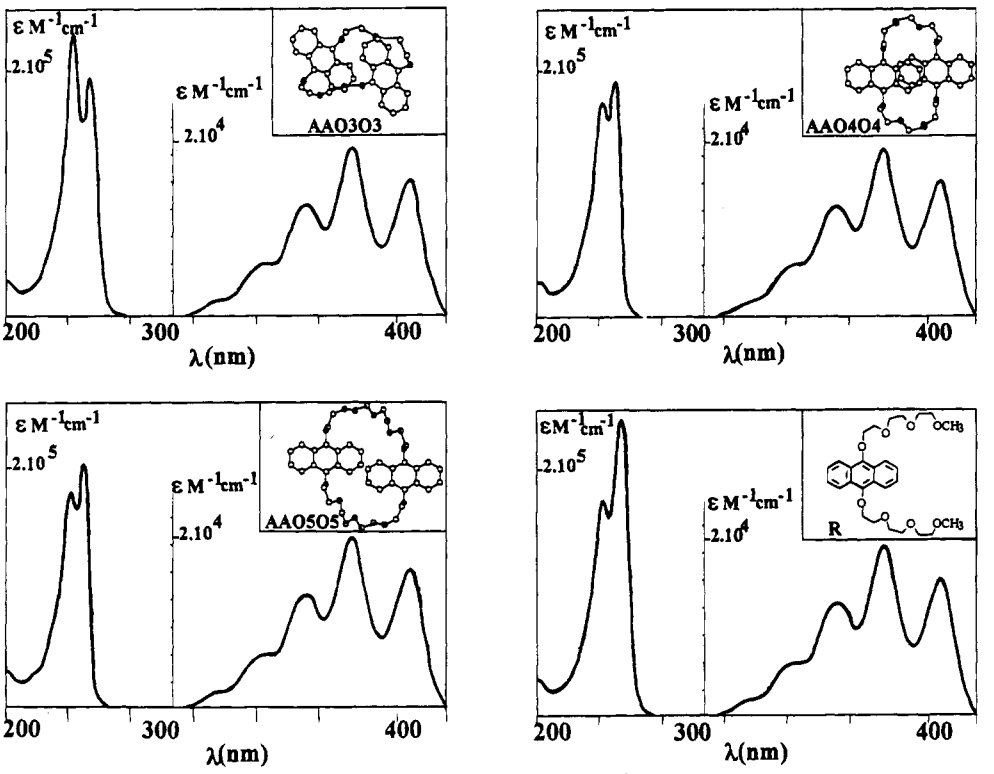

Figure 1. Electronic absorption spectra in methanol at +25 °C of coronands AAO_3O_3, AAO_4O_4, AAO_5O_5, and the reference compound R (concentration < 10^{-4} M).

istic of a 9,10-disubstituted anthracene chromophore, present slight but significant bathochromic and hypochromic shifts as compared to the reference compound R. The strongest modification occurs on the high energy and intense transition lying between 200 and 300 nm; a net redistribution of the two constituting bands is observed, revealing a mutual intramolecular interaction between the two aromatic moieties which experience some degree of parallelism in fluid solution. When shorter polyether linkages are used[9] (AAO_4O_4 and AAO_3O_3), this effect is more pronounced in relation with the close vicinity of the rings as exemplified in the solid state[10] (Figure 1).

In order to get more information on AAO_5O_5 in the ground state, the spectra were recorded in three selected solvents (methylcyclohexane, methanol, and acetonitrile) over a large temperature range. The slight temperature dependence variation of the two components of the high energy transitions (≈250 nm) is comparable for AAO_5O_5 and R upon temperature change. It indicates that, within the temperature interval investigated (see Figure 2), AAO_5O_5 experiences the same sets of conformers in the ground state. Although no noticeable shifts are detected in methanol and acetonitrile, a small but continuous hypsochromic shift (≈440 cm^{-1}) is observed in methylcyclohexane upon heating, revealing a more important reorganization of the aromatic rings in this solvent than in polar solvents (Figure 2).

3. Fluorescence Emission of AAO_5O_5 (Free Ligand).[9] 3.1. Stationary Conditions. In fluid solution, AAO_5O_5 exhibits a dual fluorescence; the emission spectrum is composed of a structured part, culminating at 440 nm, assigned to the locally excited species referred

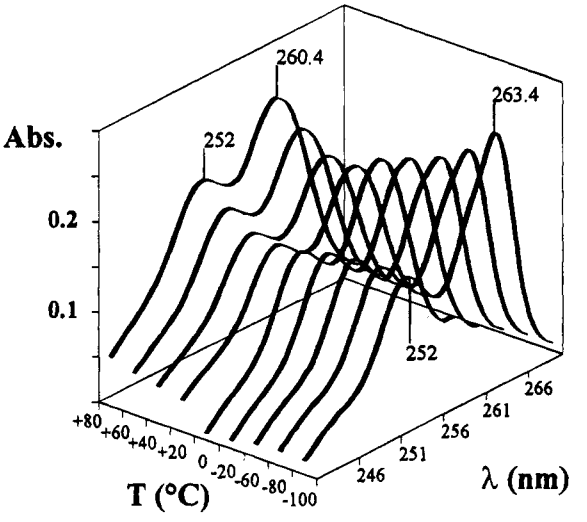

Figure 2. Electronic absorption spectra of AAO_5O_5 in methylcyclohexane (concentration < 10^{-5} M) versus temperature.

to as "monomer" (similar in shape to the reference compound R) and a red-shifted, broad and structureless band with λ_{max} = 530 nm; the latter is characteristic, in the anthracene series, of partially overlapping excimers[11] (Figure 3).

The fluorescence intensity of AAO_5O_5 was found to be markedly sensitive to the solvent polarity (Table 1). As compared to methylcyclohexane (Φ_F = 0.71) a strong fluorescence quenching was noted ($\Phi_F \approx 0.1$) for methanol and acetonitrile. Although an analogous tendency was observed for the reference compound (R), the effect is by far less intense; the origin of this important quenching

(10) Guinand, G.; Marsau, P.; Bouas-Laurent, H.; Castellan, A.; Desvergne, J.-P.; Riffaud, M.-H. *Acta Crystallogr.* **1986**, *C42*, 835–838.

(11) Ferguson, J.; Castellan, A.; Desvergne, J.-P.; Bouas-Laurent, H. *Chem. Phys. Lett.* **1981**, *78*, 446–450 and references cited therein.

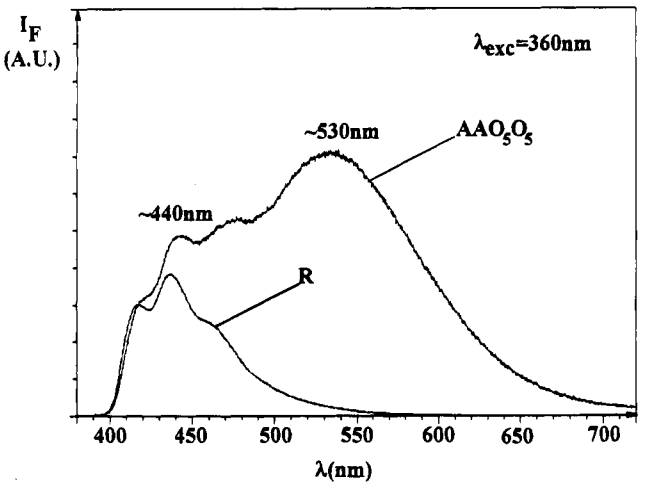

Figure 3. Corrected fluorescence emission spectrum of AAO_5O_5 and of R normalized at the first vibronic band in degassed methylcyclohexane solution at +25 °C.

Table 1. Fluorescence Quantum Yields of AAO_5O_5 (Monomer Φ_M and Excimer Part Φ_E; $\Phi_T = \Phi_M + \Phi_E$) and of the Reference Compound (R) (Φ_F) in Several Degassed Solvents at +20 °C (10^{-5} M)

solvent	Φ_M	Φ_E	Φ_T	Φ_F
methylcyclohexane	0.17	0.54	0.71	0.71
methanol	0.03	0.06	0.09	0.65
acetonitrile	0.07	0.06	0.13	0.69

should be found in the polar interactions (mainly H bonds) between the solvent and the ethyleneoxy units, especially efficient for the coronand, which maintains the solvent molecules close to the aromatic rings, thus favoring nonradiative deactivation channels.

Cooling the diluted solutions of AAO_5O_5 generates an increase of the fluorescence intensity concomitant with the diminution of the excimer contribution (Figure 4).

When the kinetic Birks[12] scheme applies, the classical Stevens Ban approximation for the fluorescence variations[13] as a function of temperature allows the determination of ΔE and ΔH, the excimer formation and stability energy, respectively. But this would be an oversimplification here because AAO_5O_5 fluorescence does not fit the Birks model as shown by transient kinetic analysis (see *infra*).

3.2. Nonstationary Regime. The time-dependent fluorescence intensities $I_F(t)$ were recorded at 410 and 560 nm, which correspond to the locally excited and excimer species emission, respectively. At 410 nm, the fluorescence emission decay is well fitted by a sum of three exponentials above a critical temperature (+10 °C in methylcyclohexane, +10 °C in acetonitrile, 0 °C in methanol) and a sum of two exponentials below this temperature. In the excimer region (560 nm), the fluorescence emission decay is satisfactorily adjusted with a sum of three exponentials below a critical temperature (+30 °C in methylcyclohexane, +30 °C in acetonitrile, 0 °C in methanol) and a sum of two exponentials above this temperature (Figure 5).

The fluorescence emission decay is clearly not compatible with the Birks[12] classical scheme depicting excimer formation, where the "monomer" decay is fitted with a sum of two exponentials and the excimer decay by a difference of two exponentials with identical kinetic parameters. In the present case, it is shown that the fluorescence decay can be adequately described by a kinetic scheme involving two distinguishable sets of monomers M_1 and M_2 and one excimer species E, the shorter lifetime monomer M_2 leading to E (Scheme 2).

That scheme is corroborated by the excitation spectra which were found to be slightly different when scanned at 560 or 410 nm, the formation of E occurring, at least in part, from a specific ground state conformer.

3.3. Interpretation of Fluorescence Measurements within Scheme 2. The interpretation of the fluorescence decays was achieved using the following simplified expressions of eq 1 and eq 2 (already shown by others to be suitable to such a situation[14]), which only apply *at low temperatures* where k_{2E} and k_{12} are supposed to be negligible versus k_E and $k_{E2} + k_M$, respectively. The fluorescence emission intensity decays of the locally excited species $I_M(t)$ and excimer species $I_E(t)$, were demonstrated to be, respectively:

$$I_M(t) \approx X_1[1 + k_{21}/(k_{E2} - k_{21})] \exp[-(k_{21} + k_M)t] + [X_2 - X_1 k_{21}/(k_{E2} - k_{21})] \exp[-(k_{E2} + k_M)t] \quad (1)$$

$$I_E(t) \approx [X_1 k_{21}/(k_M + k_{21} - k_E) + (X_2 k_{E2} - k_{21})/(k_M + k_{E2} - k_E)] \exp[-k_E t] + (X_2 k_{E2} - k_{21})/(k_E - k_M - k_{E2}) \exp[-(k_{E2} + k_M)t] + X_1 k_{21}/(k_E - k_M - k_{21}) \exp[-(k_{21} + k_M)t] \quad (2)$$

k_{M1} and k_{M2} are assumed to be identical and equal to k_M, and X_1 and X_2 are taken as the relative weight of the M_1 and M_2 populations.

The decay observed above the critical temperature on the excimer (λ_{em} = 560 nm) part is interpreted as biexponential because M_1 and M_2 behave as a single species, M_1 being rapidly transformed into M_2. Excimer E is accordingly formed from the shorter lived component M_2. From the lifetime measurements $1/\lambda_1$, $1/\lambda_2$, and $1/\lambda_3$, the rate constants k_i, listed in Table 2, can be obtained *at low temperature* using Scheme 2. Plotting ln(k) versus $1/T$ yields a linear relation (Figure 6) from which the preexponential factors k°_{21}, k°_{E2}, k°_E and the corresponding activation energy E_a can be readily deduced in methylcyclohexane and in methanol (Table 2).

The kinetic constants show that the excimer formation at +20 °C ($k_{E2} = 1.3 \times 10^8$ s^{-1} in methylcyclohexane), ($k_{E2} = 5.2 \times 10^8$ s^{-1} in methanol) is the efficient step when the locally excited species M_2 is formed, probably because its geometrical conformation is close to that of the excimer. Similar values were observed for α,ω-bis(9-anthryl)polyoxaalcanes,[16] well known for their efficient folding and remarkable flexibility.[15] Such kinetic values

(12) Birks, J. B. *Photophysics of Aromatic Molecules*; Wiley Interscience: New York, 1970.

(13) (a) Stevens, B.; Ban, M. I. *Trans. Faraday Soc.* **1964**, *60*, 1515–1523. (b) In a preliminary communication, such an approach was, however, applied for AAO_5O_5 as a first approximation. The following apparent data, considered as indicative values, were obtained: ΔH and ΔE (kcal/mol): −8.1 and 21.0 (methanol); -8.9 and 17.4 (acetonitrile); −12.5 and 13.9 (methylcyclohexane); see ref 4.

(14) (a) Fages, F.; Desvergne, J.-P.; Bouas-Laurent, H. *J. Am. Chem. Soc.* **1989**, *111*, 96–102. (b) Van der Auweraer, M.; Gilbert, A.; De Schryver, F. C. *J. Am. Chem. Soc.* **1980**, *102*, 4007–4023.

(15) Geny, E.; Monnerie, L. *J. Polym. Sci. Polym. Phys. Ed.* **1979**, *17*, 147–163.

(16) (a) Desvergne, J.-P; Castellan, A.; Lesclaux, R. *Chem. Phys. Lett.* **1980**, *71*, 228–231. (b) Desvergne, J.-P; Bitit, N.; Bouas-Laurent, H. *J. Chem. Res., Synop.* **1984**, 214–215; *J. Chem. Res., Miniprint* 1901–1921. (c) For bisanthracenes containing short and very flexible chains (OCH_2O or OCH_2CH_2O), the rate constants for the deactivation process leading to the photocycloadduct (implying the folding of the chain) were

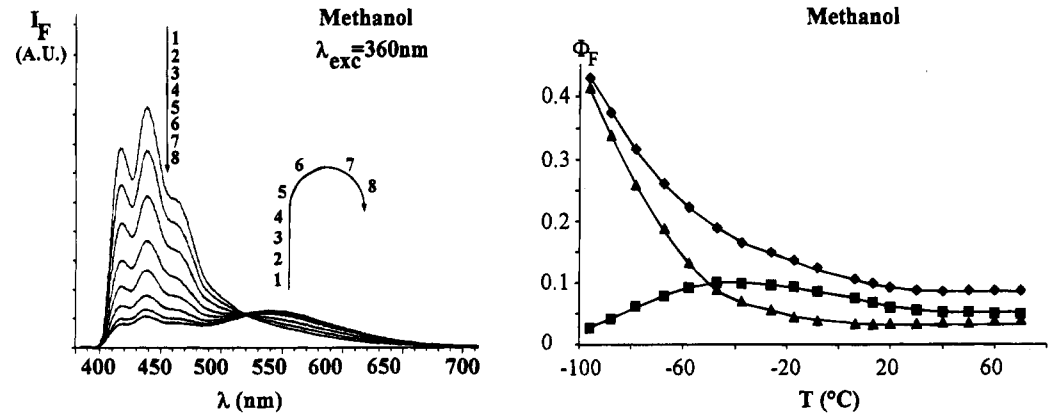

Figure 4. Corrected fluorescence emission spectra of AAO_5O_5 in methanol as a function of temperature: (1) −96 °C, (2) −88 °C, (3) −67 °C, (4) −57 °C, (5) −47 °C, (6) −37 °C, (7) −26 °C, (8) −17 °C (left). Fluorescence quantum yields versus temperature: (▲) Φ_M monomer, (■) Φ_E excimer part, (◆) Φ_G (global), λ_{exc} = 360 nm (concentration < 10^{-5} M) (right).

were found to be significantly smaller for polymethylenic sequences.[17] Activation parameters (ΔG^*, ΔH^* and ΔS^*) could be extracted for $M_1^* \rightarrow M_2^*$ from the rate constants (Table 3); the values confirm the geometrical flexibility of the receptor induced by the poly(ethylene oxide) sequences[15] since very weak activation energies were involved in the molecular folding $M_1^* \rightarrow M_2^*$ (less than 2 kcal/mol). Besides, one notes a significant negative activation entropy indicating a large conformational reorganization in both solvents. The proportion of M_1 and M_2 (X_1 and X_2) could not be determined from eqs 1 and 2 for lack of accuracy.

4. In the Presence of Cations. 4.1. Absorption and Fluorescence Spectroscopy of AAO_5O_5. As stated in a preliminary note,[3b] the spectroscopic properties of AAO_5O_5 are strongly altered in the presence of Na^+ and K^+ cations whereas no significant effects are detected for the reference compound (R). Gradual additions of Na^+ or K^+ induce a progressive change of the proportion of the two high energetic vibronic bands (≈230−250 nm) of the absorption spectrum (Figure 7, in acetonitrile).

The peculiar redistribution of these two vibronic bands is indicative of some degree of alignment of the long axes of the anthracenic moieties[18] (*vide supra*); this result suggests the shaping of the two complexing loops, holding the two chromophores at a short distance from each other. The fluorescence emission spectrum is also modified upon cation addition (Figure 8), generating progressively a new excimer band ($\lambda_{max} \approx$ 570 nm) which is different from that formed within the free ligand ($\lambda_{max} \approx$ 530 nm).

Upon stepwise addition of salt, the emission intensity of the locally excited species (~400−440 nm in acetonitrile and methanol) decreases as the emission intensity of the excimer increases. Interestingly, the same trends were observed when potassium acetate was added to a methanolic solution[19] of AAO_5O_5 even if the amplitude of the phenomenon is less intense and the maximum of the new excimer band is fairly blue-shifted (315 cm^{-1}). Upon gradual addition of $NaClO_4$, the excitation spectra of the solution scanned at 410 nm matches the absorption spectrum of the free ligand. In contrast, the excitation spectrum scanned at 560 nm resembles the UV spectrum of the Na^+-saturated solution but nevertheless shows (especially in acetonitrile) a clear contribution from the free host. It indicates that the excited complex is also partially formed from the free ligand.

Additional information was obtained from the fluorescence decay measurements (*vide infra*), but for sake of clarity, the determination of the stoichiometry is detailed first below.

5. Association Constants. The complexation process was investigated both in the ground and in the excited states. For Na^+, the application of a mathematical treatment detailed in the Experimental Section demonstrates the formation of a 2:1 stoichiometric complex, using eq 3 (eq 4 was found not to be valid), and establishes the stepwise binding constants (K_{11} and K_{12}) in both acetonitrile and methanol (Table 4).

$$\frac{A_{sol} - A_0}{A_{sol} - A_\infty} = K_{11}[M]_{tot} \frac{\alpha + K_{12}\chi[M]_{tot}}{(K_{11}[M]_{tot}(\alpha - \chi) - \chi)} \quad (3)$$

This 2:1 stoichiometry is in agreement with the structure obtained in the crystalline state[8] using X-ray diffraction techniques (Figure 9).

The stepwise and overall binding constants reveal that the constant determined in acetonitrile is larger than that in methanol. Moreover, a *positive cooperative effect* was established for Na^+ in both methanol and acetonitrile. According to a method developed by Connors,[20] this positive cooperative effect is exemplified by a Scatchard plot which presents the characteristic positive curvature (Figure 10).

The positive cooperative effect frequently encountered in biological systems[21] and in the spontaneous formation of self-assemblies such as helicates[22a,b] or other systems[22c] was less encountered for the complexation of metal

found to be (2.3−2.9) × 10^9 s^{-1} for OCH_2O and 2.0 × 10^8 s^{-1} for OCH_2-CH_2O. The corresponding activation energy for OCH_2O ΔE is equal to 3.7 kcal/mol in methylcyclohexane; that energy drops down to less than 1 kcal/mol for the isolated gas-phase excited molecule. Desvergne, J.-P; Bouas-Laurent, H.; Lahmani, F.; Sepiol, J. *J. Phys. Chem.* **1992**, *96*, 10616−10622.

(17) Castellan, A.; Desvergne, J.-P.; Bouas-Laurent, H. *Chem. Phys. Lett.* **1980**, *76*, 390−397.

(18) Hinschberger, J.; Desvergne, J.-P.; Bouas-Laurent, H.; Marsau, P. *J. Chem. Soc., Perkin Trans. 2* **1990**, 993−1000.

(19) $KClO_4$ and CH_3COONa are not soluble enough in methanol and acetonitrile for the concentrations required. For the same reasons, experiments with salts were not carried out in methylcyclohexane.

(20) Connors, K. A. *Binding Constants. The measurement of Molecular Complex Stability*; John Wiley & Sons: New York, 1987.

(21) (a) Adair, G. S. *J. Biol. Chem.* **1925**, *63*, 529−545. (b) Hill, T. L. *J. Phys. Chem.* **1953**, *57*, 324−329. (c) Steinhardt, J.; Reynolds, J. A. *Multiple equilibria in proteins*; Academic Press: New York, 1969.

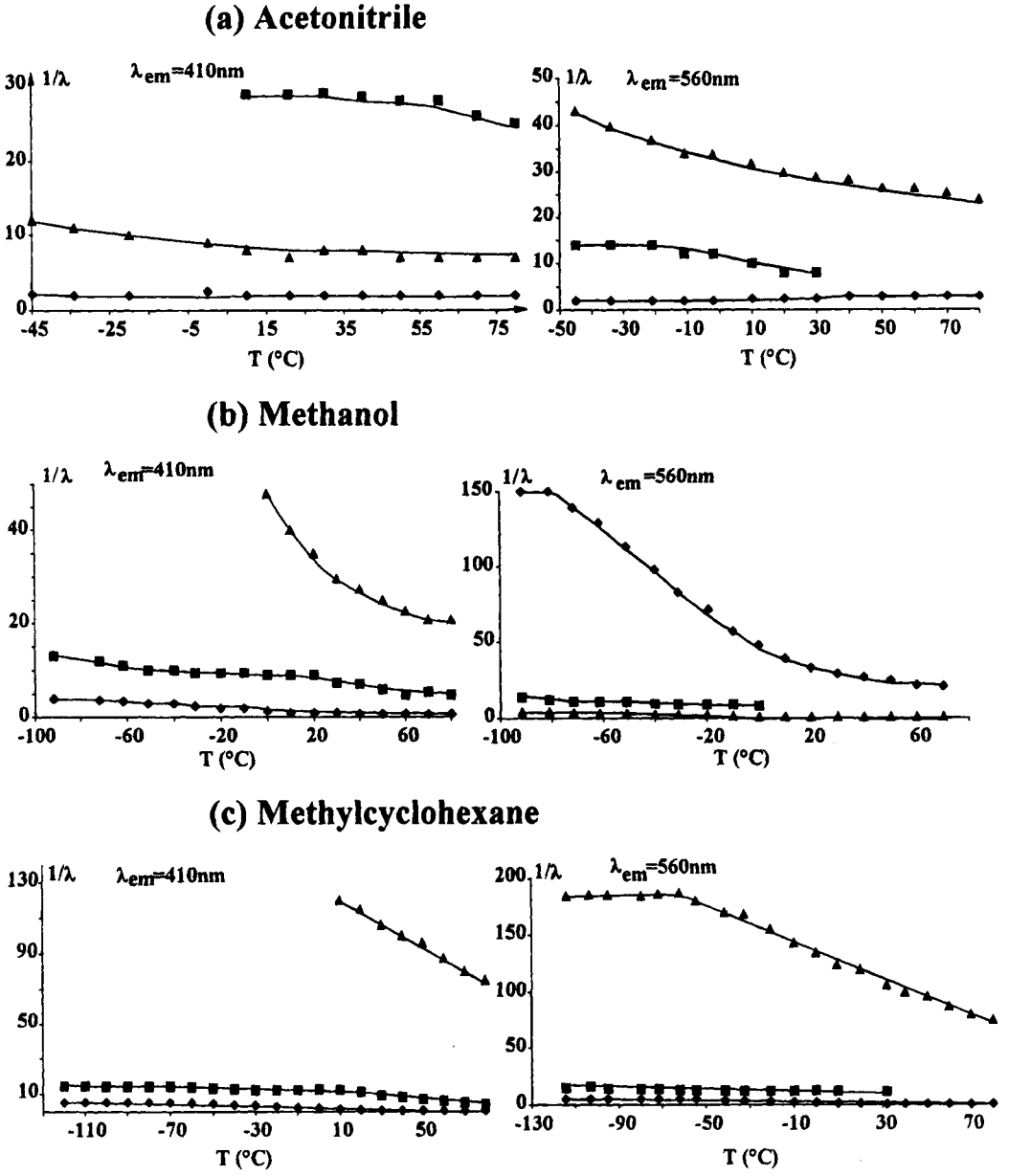

Figure 5. Kinetic parameters ($1/\lambda_i$ in ns) obtained from fluorescence emission decays of AAO_5O_5 in (a) acetonitrile, (b) methanol, and (c) methylcyclohexane measured versus temperature at 410 nm (monomer) and 560 nm (excimer) by the single photon timing technique (degassed samples $c < 10^{-5}$ M).

Scheme 2. Proposed Kinetic Scheme Describing the Formation of the Excimer E, Involving Two Distinct Ground State Conformers M_1 and M_2

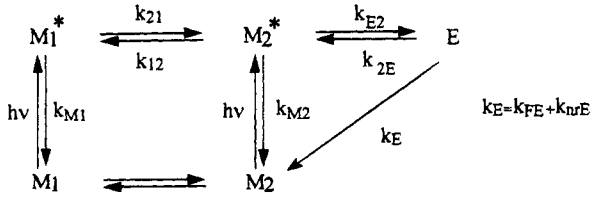

cations by crown ethers. Laszlo[22c] and Rebek[22d] observed a "negative" cooperative effect using *bicyclic* coronands. However, AAO_5O_5 has to *generate* the first coronate by coiling up around Na^+. The complexation of the first cation probably induces the preorganization of the second binding site favorable to the complexation. For the larger potassium cation (r_{K^+} = 1.33 Å versus r_{Na^+} = 0.97 Å) a 1:1 stoichiometry was found in methanol[19] using eq 4 (Table 4) (eq 3 gave $K_{21} = 0$ for K^+). That suggests that

$$\frac{A_{sol} - A_0}{A_0} = \gamma \frac{K_{11}[M]_{tot}}{1 + K_{11}[M]_{tot}} \qquad (4)$$

the second potassium cation is not complexed due to steric hindrance presented by the improper geometry of the second loop, geometry induced by the size of the first guest (Figure 11). However, the mutual orientation of the anthracenes in the K^+ 1:1 complex should not be very different from that prevailing with Na^+, as only a moderate blue-shift (315 cm^{-1}) of the excimer emission occurs.

In the ground state, as expected, the overall binding constant β (for Na^+) is larger in acetonitrile than in

(22) (a) Pfeil, A.; Lehn, J.-M. *J. Chem. Soc., Chem. Commun.* **1992**, 838–840. (b) Garret, T. M.; Koert, U.; Lehn, J.-M. *J. Org. Chem.* **1992**, *5*, 529–532. (c) Bouquant, J.; Delville, A.; Grandjean, J.; Laszlo, P. *J. Am. Chem. Soc.* **1982**, *104*, 686–691. (d) Rebek, J.; Costello, T.; Marshall, L.; Wattley, R.; Gadwood, R. C.; Onan, K. *Ibid.* **1985**, *107*, 7481–7487.

Table 2. Kinetic Parameters for the Conversion of Conformer M_1 to Conformer M_2 in the Singlet Excited State (k_{21}), Intramolecular Excimer Formation from Conformer M_2 (k_{E2}), and Decay of the Excimer of AAO_5O_5 (k_E) in Methylcyclohexane and Methanol Extrapolated at +20 °C[a]

	methylcyclohexane	methanol
k_{21} (s^{-1})	2.2×10^7	8.8×10^7
k°_{21} (s^{-1})	3.1×10^8	1.7×10^9
E_a (kcal/mol)[b]	1.55	1.7
k_{E2} (s^{-1})	1.3×10^8	5.2×10^8
k°_{E2} (s^{-1})	1.3×10^8	3.1×10^9
E_a (kcal/mol)[b]	negligible	1.0
k_E (s^{-1})	6.0×10^6	1.4×10^7
k°_E (s^{-1})	6.6×10^6	6.0×10^7
E_a (kcal/mol)[b]	negligible	negligible

[a] The deactivation rate constant of the reference compound R in the singlet excited state k_M ($1/\tau$) is 7.1×10^7 s^{-1} in methylcyclohexane and in methanol at +20 °C. The data were not determined in acetonitrile due to the scarcity of experimental values. [b] 1 cal = 4.18 J.

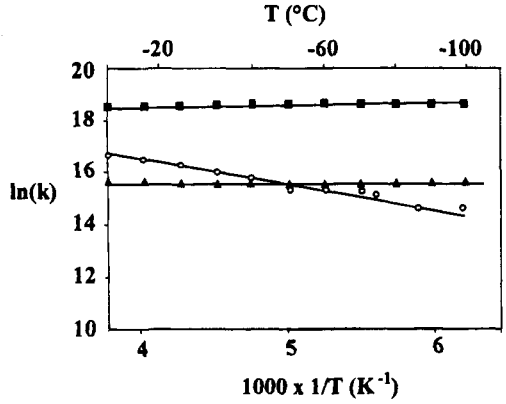

Figure 6. Arrhenius plot of the logarithm of the rate constants ($\ln k_i$) in methylcyclohexane: (○) $\ln(k_{21})$, (■) $\ln(k_{E2})$; (▲) $\ln(k_E)$ (related to Scheme 2); see Table 2.

Table 3. Activation Parameters for the Transformation $M_1^* \rightarrow M_2^*$ at 293 K[a]

solvent	ΔH^* (kcal/mol)[b]	ΔS^* (cal/mol/K)[b]	ΔG^* (kcal/mol)[b]
methylcyclohexane	1.0	−22	7.3
methanol	1.1	−18	6.5

[a] ΔH^* and ΔS^* were obtained from E_a and the frequency factor k°_{21} ($k_{21} = k^\circ_{21} \exp(-E_a/RT)$, see Table 2) using the relations $\Delta H^* = E_a - RT$ and $\Delta S^* = R[\ln(k^\circ_{21}) - \ln(RT/Nh) - 1]$ where N represents the Avogadro number, h the Planck constant, and $\Delta G^* = \Delta H^* - T\Delta S^*$. At 293 K $k^\circ_{21} = 3.15 \times 10^8$ s^{-1} (methylcyclohexane) and 1.7×10^9 s^{-1} (methanol). [b] 1 cal = 4.18 J.

methanol, the solvating ability of the alcohol being higher than that of the nitrile.

Fluorescence data gave, as compared to UV titrations, similar binding constants in methanol for both cations Na^+ and K^+. However, if in acetonitrile the positive cooperative effect is maintained, the overall binding constant β (for Na^+) is significantly larger (≈3 fold, Table 4). The determination of the stepwise binding constants indicates that K_{11} remains nearly unchanged in contrast to K_{12} which is appreciably enhanced (≈ factor 2). This discrepancy could be related to the emergence of long-lived (*vide infra*) conformers in the excited state (excimers) displaying a higher binding behavior: *i.e.*, the excimer formation, in bringing the anthracene rings closer to each other, presumably templates the formation

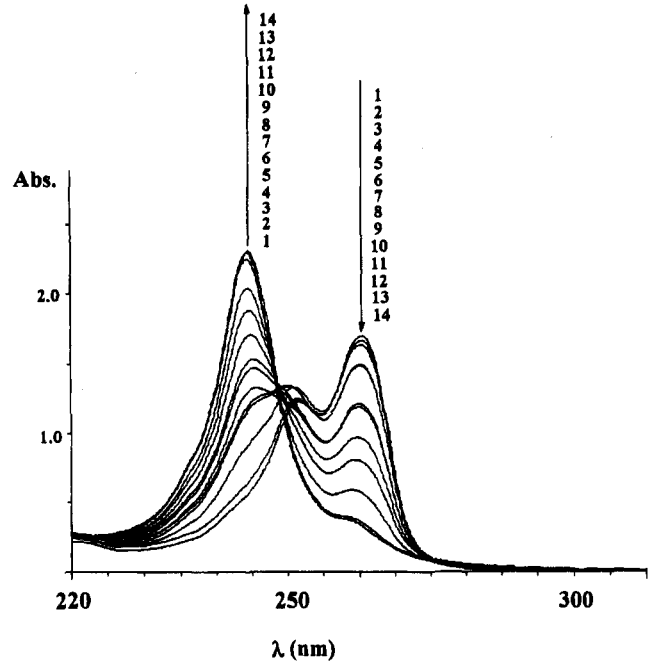

Figure 7. UV titration of AAO_5O_5 (10^{-5} M) with $NaClO_4$: (1) 0 M, (2) 5×10^{-4} M, (3) 1.25×10^{-3} M, (4) 2.5×10^{-3} M, (5) 3.25×10^{-3} M, (6) 3.75×10^{-3} M, (7) 5×10^{-3} M, (8) 7.5×10^{-3} M, (9) 10^{-2} M, (10) 2.5×10^{-2} M, (11) 5×10^{-2} M, (12) 10^{-1} M, (13) 2×10^{-1} M, (14) 1.2 M in acetonitrile. Similar titration curves were recorded for $NaClO_4$ and CH_3COOK, respectively, in methanol.

of the second complex still more efficiently than in the ground state. Further, the excimer geometry must stabilize the biscoronate. In methanol such an effect is strongly reduced for the reasons stated above.

6. Fluorescence Decay in the Presence of Cations. Upon cation addition (Na^+ or K^+), the fluorescence decay profile recorded in the excimer region was well fitted at room temperature with a sum of two exponentials. For the free ligand, however, two exponentials and three exponentials functions were required in acetonitrile and methanol, respectively. As the concentration of salt increases, the long-lived component grows up and reaches a plateau for large amounts of cations (30 → 184 ns in acetonitrile with $NaClO_4$, 40 → 165 ns in methanol with $NaClO_4$, and 40 → 215 ns in methanol with CH_3COOK, see Figure 12).

This long decay was assigned to the radiative deactivation of a more symmetrical excimer ($\lambda_{max} \approx 570$ nm, $\bar{\nu}_{max} = 17\,544$ cm^{-1}) progressively formed as the concentration of cations augments. With K^+, the 1:1 complex displays a longer fluorescence decay for a similarly shaped excimer ($\lambda_{max} \approx 560$ nm, $\bar{\nu}_{max} = 17\,857$ cm^{-1}) the excimer maximum is blue shifted by ≈315 cm^{-1} from that of the Na^+ excimer. The relative decrease of the excimer lifetime in methanol with Na^+ (165 ns) as compared to K^+ (215 ns) might be ascribable, at least in part, to the quenching influence of ion pairs which should be more efficient for the biscoronate ($2NaClO_4$) than the monocoronate (CH_3COOK).[23]

The shorter lifetime component (20 ns) that slowly decreases to zero with increasing salt concentration could be due to the nonsymmetrical excimer prevailing in the free ligand. That species progressively disappears to

(23) McCullough, J. J.; Yeroushalmi, S. *J. Chem. Soc., Chem. Commun.* **1983**, 254–255.

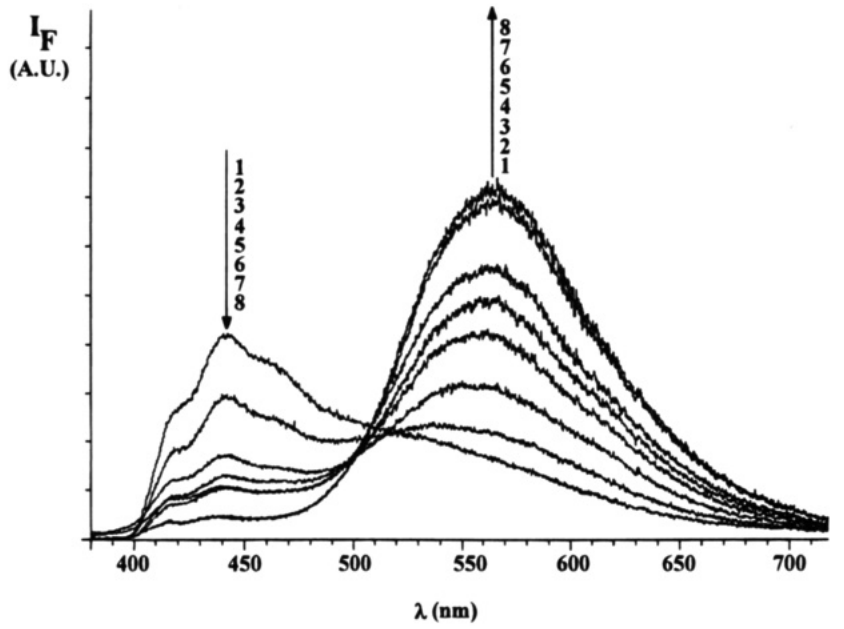

Figure 8. Fluorescence emission titration of AAO_5O_5 (5×10^{-6} M) with $NaClO_4$ in degassed acetonitrile at +25 °C (λ_{exc} = 360 nm): (1) 0 M, (2) 10^{-3} M, (3) 2×10^{-3} M, (4) 3×10^{-3} M, (5) 4×10^{-3} M, (6) 5×10^{-3} M, (7) 5×10^{-2} M, (8) 0.1 M.

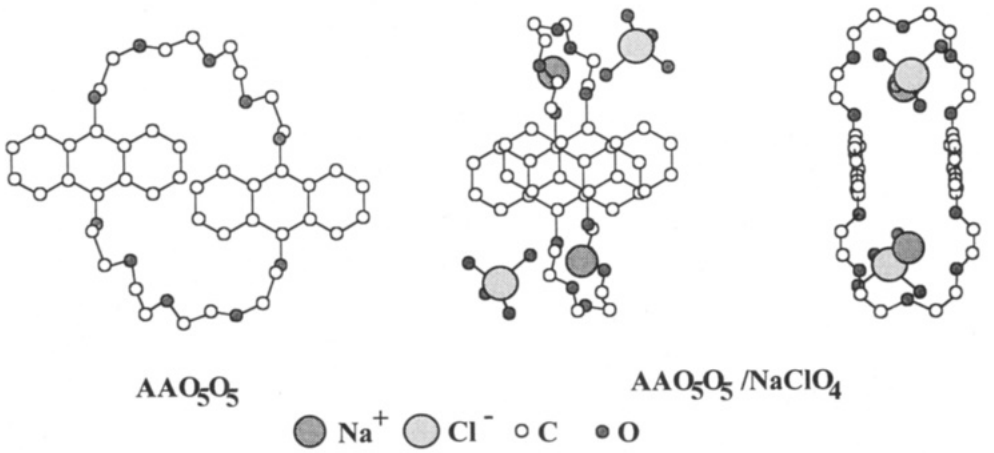

Figure 9. Molecular conformation (ball and stick) of the free ligand AAO_5O_5 and the binuclear complex AAO_5O_5/$NaClO_4$ in the crystal[8] (the size of Na^+ and chlorine atom were exaggerated for clarity).

Table 4. Evaluation of the Binding Constants (Accuracy ±10%) Using UV Spectroscopy (GS = Ground State) and Fluorescence Emission Spectroscopy (ES = Excited State)[a]

salt/solvent		β^a	K_{11} (M^{-1})	K_{12} (M^{-1})
$NaClO_4$/acetonitrile	GS	37 000	178	236
	ES	100 000	200	500
$NaClO_4$/methanol	GS	118	3	42
	ES	115	*b*	*b*
CH_3COOK/methanol	GS	9	9	
	ES	10	10	

[a] Na^+: β (M^{-2}). K^+: β (M^{-1}). [b] Values were not determined.

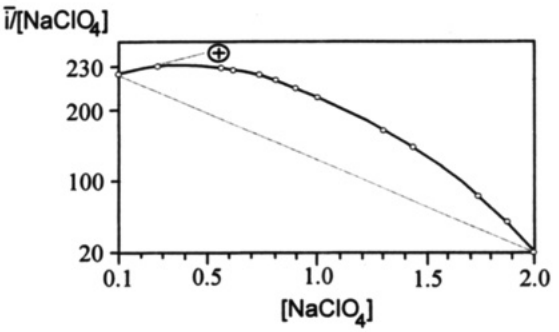

Figure 10. Scatchard plot: $\bar{i}$/[$NaClO_4$] (○) versus [$NaClO_4$] (mol/L) from titration of AAO_5O_5 with $NaClO_4$ (in acetonitrile at +25 °C from UV data). The positive curvature for [$NaClO_4$] = 0 indicates the positive cooperativity of the two-step complexation (see Experimental Section). $\bar{i} = (K_{11} + 2K_{11}K_{12}[NaClO_4])/(1 + K_{11}[NaClO_4] + K_{11}K_{12}[NaClO_4]^2)$.

form the metal-complexed excimer. The excitation spectrum scanned at 560 nm (symmetrical excimer) demonstrates the participation of the free ligand to the formation of the metal complexed excimer since it includes the contribution of both free and complexed species. In contrast, the excitation spectrum monitored on the locally excited species (≈410 nm) matches only the free ligand which discards the decomplexation of the metal complexed excimer in the excited state toward the free ligand (that point is confirmed by fluorescence decay measurements on the locally excited part, at ≈410 nm, which do not present any significant contribution from long lifetime components obtained at 560 nm). The detailed kinetic study of the metal complexed species in the excited state was not pursued due to the complexity of

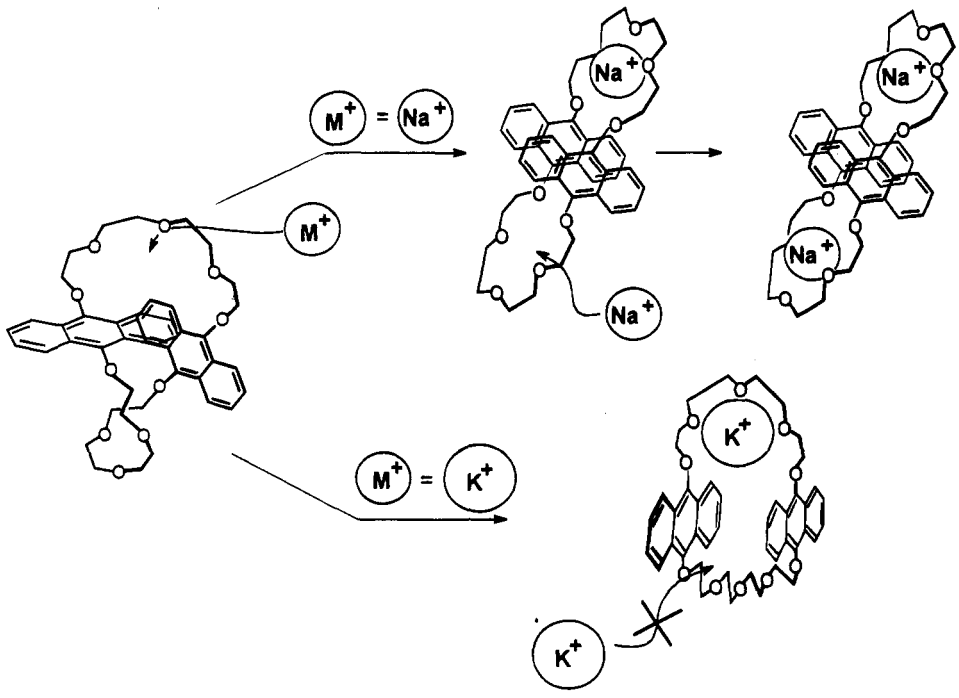

Figure 11. Proposed scheme for the complexation of Na^+ and K^+ by AAO_5O_5.

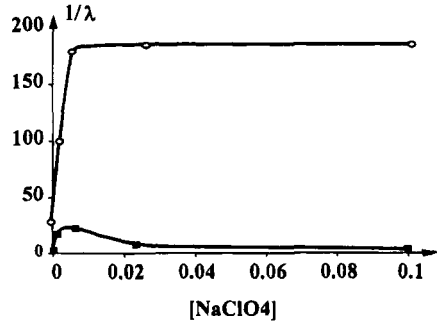

Figure 12. Decay parameters ($1/\lambda_i$) obtained from fluorescence lifetime measurements on the excimer part (560 nm) of AAO_5O_5 in the presence of increasing concentrations of $NaClO_4$ in degassed solutions of acetonitrile at room temperature. Very similar diagrams were obtained for $NaClO_4$ and CH_3COOK in methanol.

Table 5. Photocycloaddition Quantum Yields (Φ_R) for the Disappearance of AAO_5O_5 in Degassed Solvents in the Absence or Presence of Cations ($NaClO_4$ or CH_3COOK) in Large Excess at Room Temperature. On Account of the Thermal Reverse Reaction, the Data in the Presence of Salts Are Minimum Values

solvent salt	Φ_R
acetonitrile	2.7×10^{-4}
acetonitrile ($NaClO_4$)	4.2×10^{-3}
methanol	1.9×10^{-4}
methanol ($NaClO_4$)	8.3×10^{-3}
methanol (CH_3COOK)	1.8×10^{-3}

the fluorescence decays at ≈410 nm which did not present any straighforward relation with that recorded at 560 nm.

Temperature Dependence. Plotting the logarithm of the overall binding constant β ($\ln \beta$), calculated with Na^+ in acetonitrile in the excited state, versus $1/T$ gave a straight line from which the thermodynamic parameters ΔH and ΔS could be extracted (Figure 13).

These are overall values indicating a larger stability of the biscoronate than the free ligand (negative enthalpy) and a more ordered system (negative entropy) as expected from the known structures. Nevertheless, a complete analysis requires data for K_{11} and K_{12} which could not be obtained due to experimental difficulties.

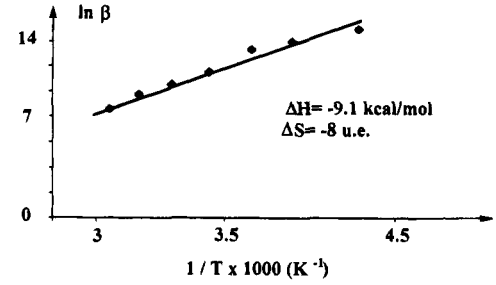

Figure 13. Plots of $\ln \beta$ versus $1/T$ in the excited state (where β is the global binding constant of AAO_5O_5 toward Na^+ in acetonitrile). ΔH (1 cal = 4.18 J) and ΔS 1 ue = 1 cal·mol^{-1}·K^{-1} were obtained from the slope and the intercept of the curve.

7. Photoreactivity. Upon irradiation, AAO_5O_5 was found to be reactive in the presence or in the absence of cation (Na^+ or K^+). The process is independent of the concentration (10^{-6}–10^{-4} mol/L), proving its intramolecular nature. The UV spectrum revealed the disappearance of the long wavelength absorption band (320–420 nm) characteristic of the anthracene moiety in three selected solvents (diethyl ether, acetonitrile, methanol) with or without salts. Moreover, a net increase of the reaction quantum yield is recorded in the presence of cations (Table 5).

Without cation, the sole photoproduct formed (Pd) was isolated from a degassed diethyl ether solution; its structure, dissymmetrical, involves the 9,10–1′,4′ vertices of the anthracene parts (Figure 14) as established by NMR and UV spectroscopy (naphthalenic absorption, see Experimental Section).

This result is in keeping with the unsymmetrical geometry of the fluorescent excimer ($\lambda_{max} \approx 530$ nm) assumed to be on the reaction pathway. In acetonitrile without salt, spectroscopic considerations (UV and fluo-

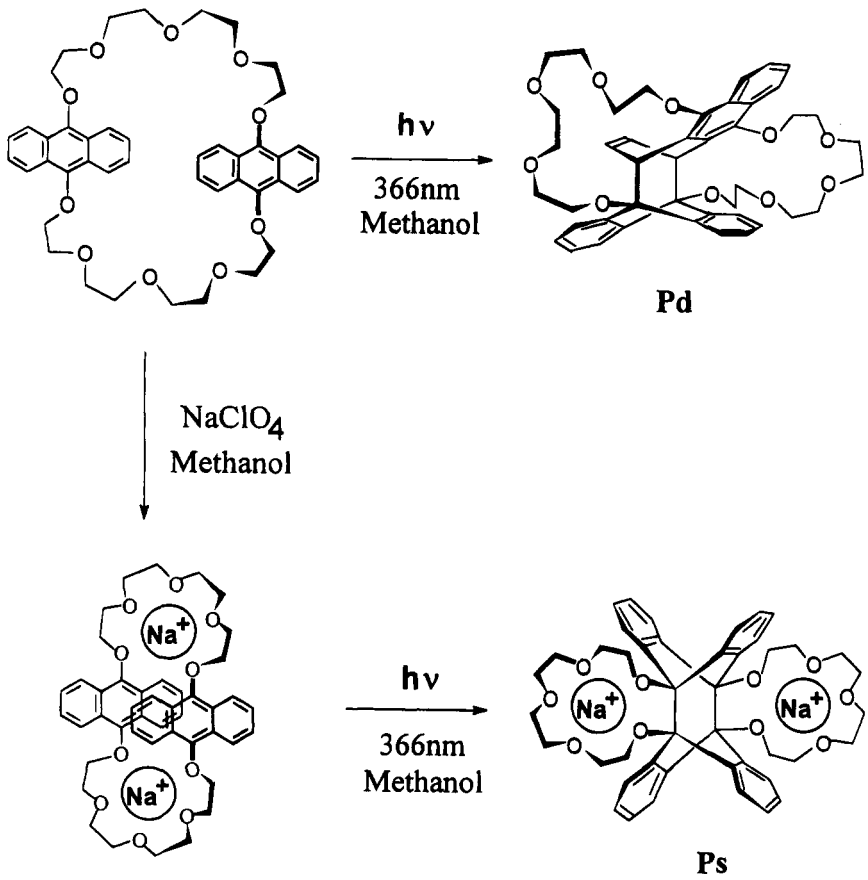

Figure 14. Schematic representation of the formation of the photoproducts Pd and Ps without and with Na^+.

rescence emission) indicate that the same dissymmetrical photoproduct (Pd) is formed. In the presence of Na^+, another photocycloadduct, Ps, was generated. Ps is not thermally stable, slowly reverting to the starting material at room temperature. Its structure could be deduced from the UV absorption spectrum of an irradiated methanolic solution saturated by $NaClO_4$, which was found to be characteristic of the 9,10−9′,10′ planosymmetric anthracene photodimer[2] (see Experimental Section); its geometry is in accordance with the intermediacy of the symmetrical excimer peaking at 570 nm. With K^+ in methanol, the spectrum resembles that obtained with Na^+, suggesting the formation of the same photoproduct (Ps) originating from a similarly shaped excimer. Although K^+ also templates the formation of the symmetrical photoproduct (Ps) (*vide supra*), the reaction efficiency is lower ($\Phi_{RNa^+} \approx 8.3 \times 10^{-3}$, $\Phi_{RK^+} \approx 1.8 \times 10^{-3}$) probably in relation with a higher steric hindrance. As represented in Figure 14, the influence of cations on the photodimerization induces a complete change of regioselectivity, a clear example of cation-directed photochemistry. Nevertheless, the quantum yields are low, presumably on account of steric constraints in transforming the excimers into photodimers. This is the reason why the photochemical reactivity of AAO_5O_5 was not further investigated.

Conclusion. Monocyclic coronands incorporating two 9,10-anthracenediyl groups have been described. It was shown that AAO_5O_5 behaves as a photoresponsive supramolecular system capable of directing photochemistry by cation complexation. It undergoes a profound conformational reorganization by wrapping itself around Na^+ and forming a biscoronate; consequently, one observes a complete change of intramolecular *photocycloaddition regiospecificity* between the free ligand and the 2:1 complex. It is a clear-cut example of the influence of cation complexation upon photochemistry. Moreover, the system has *photochromic* properties, but the low quantum yield of the photochemical step prevents consideration for utilization in a photochromic device.

The fluorescence of AAO_5O_5, sensitive to the nature of the solvent, was also found to be strongly dependent on the nature and concentration of metal cations. *The distinct influence of Na^+* upon the *wavelength, intensity, and lifetime of the excimer* (from free ligand to biscoronate, in methanol: $\Delta\bar{\nu} = 1350$ cm^{-1}, intensity multiplied by 3, $\tau = 23$ ns to 165 ns) should be noted. This suggests a possible application for cation driven frequency converter device.

Finally, one should stress the observation of a *positive cooperative effect* in the binding of two sodium cations in the ground state and, remarkably, also in the excited state. This result is in contrast with the previous reports by others of "negative" cooperative effects for bicyclic coronands. In the present case, the entropy factor should play a critical role as the system has to build up a receptor by coiling up around the cations.

Experimental Section

General Methods. Solvents for synthesis were dried [THF (from Na/benzophenone ketyl), DMF (from CaH_2), and MeCN (from P_2O_5)] according to standard procedures. The *fluorescence quantum yields* were determined by comparison with quinine sulfate in 1 N sulfuric acid ($\Phi_F = 0.55$). The *reaction quantum yields* were determined using the Parker method.[24]

(24) Hatchard, C. G.; Parker, C. A. *Proc. R. Soc. London* **1956**, *A235*, 518−536.

Spectroscopic grade solvents were used for spectrophotometric measurements. No fluorescent contaminants were detected upon excitation in the wavelength region of experimental interest. The samples (concentration < 10^{-5} M) were degassed by freeze–pump–thaw cycles on a high-vacuum line and sealed under vacuum. The *temperature-dependent measurements* (UV and fluorescence) were performed using a quartic cell, 1 cm optical pathlength, placed in a copper holder inside a quartz Dewar flushed by cold nitrogen gas. The temperature (±0.5 °C) monitored by a platinum temperature sensor was adjusted by the nitrogen flow. *Fluorescence decay measurements* were performed using the single-photon timing technique as already described.[25] The experimental decay profiles were fitted using the Decan 1.0 program.[26] The quantum yield (fluorescence, reaction, ...) and lifetimes were determined with an *accuracy of approximately 10%*.

1,13-Ditosyl-1,4,7,10,13-pentaoxatridecane.[27] Sodium hydroxide (6.0 g, 150 mmol) dissolved in H_2O (30 mL) and tetraethylene glycol (10.0 g, 52 mmol) dissolved in THF (30 mL) were cooled down to 0–5 °C in an ice bath with stirring. Toluene-*p*-sulfonyl chloride (19.2 g, 100 mmol) in THF (30 mL) was added dropwise to the mixture over 2 h with continuous stirring and cooling. The solution was stirred vigorously for an additional 2 h before being poured into ice–water (100 mL). The ditosylate was isolated by extracting twice with CH_2Cl_2 (60 mL). The combined organic extracts were washed twice with H_2O (60 mL) and once with a saturated aqueous sodium chloride solution (60 mL) and then dried ($CaCl_2$). Removal of the solvent afforded 1,13-ditosyl-1,4,7,10,13-pentaoxatridecane as a yellow oil (22.7 g, 87%): ^{1}H NMR ($CDCl_3$, 200 MHz) δ 2.23 (6 H, s), 3.36 (8 H, s), 3.36–4.20 (8 H, m), 7.23–7.53 (4 H, m), 7.63–7.96 (4 H, m). The ditosylate was used without further purification.

1,10-Ditosyl-1,4,7,10-tetraoxadecane.[27] Pyridine (250 mL) and triethylene glycol (60 g, 0.4 mol) were cooled to 0 °C in an ice bath, under argon, with stirring. Toluene-*p*-sulfonyl chloride (160 g, 0.8 mol) was added in small portions over 2 h with continuous stirring at 0 °C. The solution was stirred vigorously for 8 h at 0 °C before being poured into ice–water (500 mL) acidified with concentrated HCl (20 mL). The compound which precipitated was filtered, washed with water, and dried over P_2O_5. Crystallization from ethanol afforded 1,7-ditosyl-1,4,7,10-tetraoxadecane (137 g, 74%) as white crystals: mp 79 °C (lit.[27] mp 78 °C); ^{1}H NMR ($CDCl_3$, 200 MHz) δ 2.23 (6 H, s), 3.33 (8 H, s), 3.33–3.40 (4 H, m), 7.10–7.46 (4 H, m), 7.56–7.90 (4 H, m). The bistosylate was used without further purification.

1,7-Ditosyl-1,4,7-trioxaheptane.[27] Pyridine (240 mL) and diethylene glycol (42.4 g, 0.4 mol) were cooled to 0 °C in an ice bath, under argon, with stirring. Toluene-*p*-sulfonyl chloride (192 g, 1 mol) was added in small portions over 2 h with continuous stirring at 0 °C. The solution was stirred vigorously for 8 h at 0 °C before being poured into ice–water (500 mL) acidified with concentrated HCl (20 mL). The compound which precipitated was filtered, washed with water, and dried over P_2O_5. Crystallization from ethanol afforded 1,7-ditosyl-1,4,7-trioxaheptane (140.8 g, 85%) as white crystals: mp 98 °C (lit.[27] mp 98 °C).

1,13-Diiodo-1,4,7,10,13-pentaoxatridecane.[6] Tetraethylene glycol ditosylate (100.5 g, 0.2 mol) and NaI (150 g, 1.0 mol) in acetonitrile (2 L) were heated under reflux for 20 h. After filtration, acetonitrile was removed *in vacuo*. Water (200 mL) was added to the residue, and the oil which separated was extracted three times with $CHCl_3$ (200 mL). The combined organic extracts were washed with H_2O (100 mL) and concentrated *in vacuo*. The residue was dissolved in toluene (200 mL) and dried ($CaCl_2$). The solution was concentrated *in vacuo* to afford 1,13-diiodo-1,4,7,10,13-pentaoxatridecane as a yellow oil (72.9 g, 88%): bp 149–150 °C/0.1 Torr; ^{1}H NMR ($CDCl_3$, 200 MHz) δ 3.95 (8 H, s), 3.40–3.80 (4 H, m), 3.80–4.33 (4 H, m). The compound was used without further purification.

1,10-Diiodo-1,4,7,10-tetraoxadecane.[6] 1,10-Ditosyl-1,4,7,-10-tetraoxadecane (32 g, 70 mmol) and NaI (41 g, 280 mmol) in acetone (400 mL) were stirred under argon at room temperature for 5 days. After filtration, acetone was removed *in vacuo* and the remaining yellow solid was extracted twice with CH_2Cl_2 (250 mL). The organic extracts were washed with a saturated $Na_2S_2O_3$ solution and dried over Na_2SO_4. The solution was concentrated *in vacuo* to afford 1,10-diiodo-1,4,7,-10-tetraoxadecane as a yellow oil (22 g, 85%) which was stored protected from light over molecular sieves (4 Å): bp 110–111 °C/0.3 Torr (lit.[6] bp 100–101 °C); ^{1}H NMR ($CDCl_3$, 90 MHz) δ 3.33–3.80 (4 H, m), 3.93 (4 H, s), 3.80–4.23 (4 H, m). The compound was used without further purification.

1,7-Diiodo-1,4,7-trioxaheptane.[6] 1,7-Ditosyl-1,4,7-trioxaheptane (33.4 g, 80 mmol) and NaI (48 g, 320 mmol) in acetone (300 mL) were stirred under argon at room temperature for 5 days. After filtration, acetone was removed *in vacuo* and the remaining yellow solid was extracted twice with CH_2Cl_2 (200 mL). The organic extracts were washed with a saturated $Na_2S_2O_3$ solution and dried over Na_2SO_4. The solution was concentrated *in vacuo* to afford 1,7-diiodo-1,4,7-trioxaheptane as a yellow oil (21.6 g, 83%) which was stored in the dark over molecular sieves (4 Å): bp 100–101 °C/0.1 Torr (lit.[6] bp 100–101 °C); ^{1}H NMR ($CDCl_3$, 90 MHz) δ 3.56–4.07 (4 H, m), 4.07–4.50 (4 H, m). The compound was used without further purification.

9,10-Bis(trimethylsiloxy)anthracene[28] **(A, Scheme 1).** 9,10-Anthraquinone (2.08 g, 10 mmol) was dissolved in dry THF (170 mL) at room temperature under argon, in the presence of magnesium powder (0.48 g, 20 mmol), and trimethylchlorosilane (8.69 g, 80 mmol) was added with stirring. DMSO (5 mL) was added to increase the polarity of the mixture which was heated under reflux for 2 h. Then, the solution was concentrated *in vacuo* and the solid residue was extracted with hexane, from which it crystallized at low temperature (0 °C) to afford 9,10-bis(trimethylsiloxy)anthracene (3.26 g, 92%): mp 124–125 °C (lit.[5a] mp 123–125 °C) (lit.[28] 124–125 °C); FABMS 354 (M^+); ^{1}H NMR ($CDCl_3$, 200 MHz) δ 0.33 (18 H, s), 7.30–7.70 (4 H, m), 8.10–8.50 (4 H, m).

9,10-Bis[(1-iodo-3,6,9-trioxaundecyl)oxy]anthracene (B, Scheme 1). K_2CO_3 (40.0 g, 0.34 mol) in acetone (150 mL) was placed in a three-necked flask under argon. After being bubbled under argon for 30 min, the mixture was heated under reflux and stirred. 1,13-Diiodo-1,4,7,10,13-pentaoxatridecane (66.0 g, 160 mmol) and 9,10-bis(trimethylsiloxy)anthracene (5.66 g, 16 mmol) in acetone (100 mL) were added dropwise simultaneously during 10 min. After being heated and stirred for 5 h, the mixture was cooled to room temperature and filtered. Column chromatography [silica gel, Et_2O–light petroleum (60–80 °C) (1:1)] afforded 9,10-bis[(1-iodo-3,6,9-trioxaundecyl)oxy]anthracene as a yellow oil (9.0 g, 72%): ^{1}H NMR ($CDCl_3$, 200 MHz) δ 3.10–3.46 (4 H, m), 3.67 (8 H, s), 3.77 (8 H, s), 3.46–4.20 (8 H, m), 4.20–4.63 (4H, m), 7.30–7.73 (4 H, m), 8.26–8.67 (4 H, m); ^{13}C NMR ($CDCl_3$) 3.4, 71.1, 72.1, 74.9, 76.6, 122.8, 125.2, 147.2; IR (KBr) $\bar{\nu}_{max}$ 3030, 2910, 2900, 2880, 1620, 1440, 1410, 1390, 1380, 1345, 1300, 1250, 1170, 1020, 990, 930, 880, 800, 770, 690 cm^{-1}; MS (70 eV) *m/z* 782 (M^+, 17), 209 (9), 155 (100). Anal. Calcd for $C_{30}H_{40}O_8I_2$: C, 46.04; H, 5.11; O, 16.37; I, 32.48. Found: C, 46.27; H, 5.15; O, 16.63; I, 32.07.

1,4,7,10,13,24,27,30,33,36-Decaoxa[13.13]-9,10-anthracenophane (AAO_5O_5). K_2CO_3 (50 g, 0.36 mol) and $CsCO_3$ (0.546 g, 0.166 mmol) in acetone (1.6 L) degassed with argon were heated under reflux. Then, a solution of 9,10-bis[(1-iodo-3,6,9-trioxaundecyl)oxy]anthracene (5.20 g, 6.65 mmol) and 9,-10-bis(trimethylsiloxy)anthracene (2.35 g, 6.65 mmol) in acetone (200 mL) protected from sunlight was added dropwise over 6 h. Heating and stirring were continued for 4 days. Then, the solution was filtered and the solvent removed *in*

(25) Desvergne, J.-P.; Bitit, A.; Castellan, A.; Bouas-Laurent, H.; Soulignac, J.-C. *J. Lumin.* **1987**, *37*, 175–181.
(26) de Roeck, T.; Boens, N.; Dockx, J. DECAN 1.0, K.U. Leuven, Belgium.
(27) Dale, J.; Kristiansen, P. O. *Acta. Chem. Scand.* **1971**, *26*, 1471–1478.
(28) Bouas-Laurent, H.; Lapouyade, R.; Brigand, C.; Desvergne, J.-P. *C. R. Acad. Sc. Paris* **1970**, *270C*, 2167–2170.

vacuo. A flash column chromatography [silica gel, Et_2O–light petroleum (60–80 °C) (1:1)] of the residue afforded 1,4,7,10,13,24,27,30,33,36-decaoxa[13.13]-9,10-anthracenophane as a yellow solid (1.46 g, 30%): mp 156 °C; ^1H NMR ($CDCl_3$, 200 MHz) δ 3.83–4.16 (8 H, m), 3.86 (16 H, s), 4.16–4.50 (8 H, m), 7.14–7.43 (4 H, m), 8.16–8.46 (4 H, m); ^{13}C NMR δ 65.8, 70.5, 71.0, 74.73, 122.5, 124.9, 125.1, 146.9; IR (KBr) $\bar{\nu}_{max}$ 3030, 2930, 2880, 1630, 1470, 1420, 1400, 1360, 1350, 1300, 1270, 1250, 1135, 1105, 1075, 950, 900, 850, 800, 770, 680 cm^{-1}; UV λ_{max} (nm) (ϵ) methylcyclohexane 251.0 (5.2×10^4), 261 (6.7×10^4), 350.0 (2.2×10^3), 364.0 (3.8×10^3), 381.5 (5.9×10^3), 402.5 (4.9×10^3); methanol 250.5 (1.6×10^5), 259.6 (1.9×10^5), 345.5 (4.6×10^3), 363.6 (1.0×10^4), 380.9 (1.6×10^4) 402.9 (1.3×10^4); acetonitrile 251.6 (1.6×10^5), 260.5 (2.2×10^5), 349.0 (5.3×10^3), 365.5 (1.1×10^4), 382.2 (1.6×10^4), 404.2 (1.3×10^4); MS (70 eV) *m/z* 736 (M^+, 38), 368 (7), 208 (32), 207 (21), 194 (17), 180 (28), 165 (10), 152 (17), 45 (100). Anal. Calcd for $C_{44}H_{48}O_{10}$: C, 71.74; H, 6.52; O, 21.74. Found: C, 71.75; H, 6.46; O, 21.97.

1,4,7,10,21,24,27,30-Octaoxa[10.10]-9,10-anthracenophane (AAO_4O_4). K_2CO_3 (50 g, 0.35 mol) and $CsCO_3$ (0.283 g, 0.87 mmol)in acetone (1.5 L) degassed with argon was heated under reflux. Then, a solution of 9,10-bis[(1-iodo-3,6,9-trioxaundecyl)oxy]anthracene (1.24 g, 3.49 mmol) and 1,10-diiodo-1,4,7,10-tetraoxadecane (2.42 g, 3.49 mmol) in acetone (200 mL) protected from sunlight was added dropwise over 30 h. Heating and stirring were continued for 4 days. Then, the solution was filtered and the solvent removed *in vacuo*. Flash column chromatography [silica gel, Et_2O–light petroleum (60–80 °C) (1:1)] of the residue afforded 1,4,7,10,21,24,27,30-octaoxa[10.10]-9,10-anthracenophane as a yellow solid (600 mg, 29%): mp 174 °C; ^1H NMR ($CDCl_3$, 90 MHz) δ 3.93 (8 H, s), 3.93–4.23 (8 H, m), 4.23–4.57 (8 H, m), 7.17–7.53 (4 H, m), 8.23–8.57 (4 H, m); ^{13}C NMR δ 70.7, 71.5, 74.72, 122.6, 124.8, 146.9; IR (KBr) $\bar{\nu}_{max}$ 3060, 2900, 2850, 1620, 1460, 1430, 1400, 1370, 1350, 1290, 1270, 1230, 1150–1050, 940, 920, 890, 790, 760, 670, 620 cm^{-1}; MS (70 eV) *m/z* 648 (M^+, 38), 368 (7), 208 (32), 207 (21), 194 (17), 180 (28), 165 (10), 152 (17), 45 (100); HRMS calcd for $C_{40}H_{40}O_8$ 648.272319, found 648.272263.

1,4,7,18,21,24-Hexaoxa[7.7]-9,10-anthracenophane (AAO_3O_3). K_2CO_3 (20 g, 0.14 mol) in acetone (650 mL) degassed with argon was heated under reflux. Then, a solution of 9,10-bis[(1-iodo-3,6,9-trioxaundecyl)oxy]anthracene (2.48 g, 7 mmol) and 1,7-diiodo-1,4,7-triooxahexane (2.28 g, 7 mmol) in acetone (200 mL) protected from sunlight was added dropwise over 6 h. Heating and stirring were continued for 4 days. Then, the solution was filtered and the solvent removed *in vacuo*. A flash column chromatography [silica gel, Et_2O–light petroleum (60–80 °C) (7:3)] of the residue (6 g) afforded 1,4,7,18,21,24-hexaoxa[7.7]-9,10-anthracenophane as a yellow solid (60 mg, 3%): mp 240 °C; ^1H NMR ($CDCl_3$, 90 MHz) δ 4.06 (16 H, s), 7.46–7.78 (4 H, m), 8.26–8.63 (4 H, m); ^{13}C NMR δ 70.5, 73.5, 122.5, 124.6, 124.8, 147.0; IR (KBr) $\bar{\nu}_{max}$ 3060, 2930, 2870, 1620, 1435, 1390, 1350, 1170, 1120, 1000, 780, 690, 670, 620 cm^{-1}; MS (70 eV) *m/z* 560 (M^+, 38), 368 (7), 208 (32), 207 (21), 194 (17), 180 (28), 165 (10), 152 (17), 45 (100); HRMS calcd for $C_{36}H_{32}O_6$ 560.219889, found 560.220318.

1-Tosyl-10-methyl-1,4,7,10-tetraoxadecane.[27] Pyridine (250 mL) and triethylene glycol monomethyl ether (82 g, 0.5 mol) in an argon atmosphere were cooled to 0–5 °C in an ice bath with stirring. Tosyl chloride (95 g, 0.5 mol) was added portionwise to the mixture over 2 h with continuous stirring and cooling. The solution was stirred vigorously for an additional 6 h and then poured into ice–water (500 mL) acidified with concentrated HCl. The precipitate was washed twice with H_2O (60 mL) and once with a saturated sodium chloride aqueous solution (60 mL) and then dried over $CaCl_2$. Removal of the solvent afforded 1-tosyl-10-methyl-1,4,7,10-tetraoxadecane as a yellow oil (148 g, 93%).

1-Iodo-10-methyl-1,4,7,10-tetraoxadecane. A mixture of sodium iodide (30 g, 0.2 mol) and 1-tosyl-10-methyl-1,4,7,10-tetraoxadecane (32 g, 0.1 mol) in acetone (400 mL) was refluxed with continuous stirring under argon for 8 h. The solvent was removed *in vacuo*, water (200 mL) was added to the residue, and the oil which separated was extracted three times with CH_2Cl_2 (200 mL). The combined organic extracts were washed with an aqueous solution of $Na_2S_2O_3$ and dried over Na_2SO_4. Removal of the solvent afforded 1-iodo-10-methyl-1,4,7,10-tetraoxadecane as a yellow oil (17 g, 62%): ^1H NMR ($CDCl_3$, 200 MHz) δ 3.20 (3 H, s), 3.50–4.00 (12 H, m); IR (KBr) $\bar{\nu}_{max}$ 1100 cm^{-1}.

9,10-Bis[(10-methyl-1,4,7,10-tetraoxadecyl)oxy]anthracene (Compound R). K_2CO_3 (13.0 g, 90 mmol) in acetone (400 mL) was placed in a three-necked flask under argon. After being bubbled under argon for 1 min, the mixture was heated under reflux with stirring. 9,10-Bis(trimethylsiloxy)anthracene (3.64 g, 10 mmol) and 1-iodo-10-methyl-1,4,7,10-tetraoxadecane (7.0 g, 25 mmol) in acetone (100 mL) were added simultaneously over 10 min. After being heated and stirred for 5 h, the mixture was cooled down to room temperature and water (200 mL) was added to the medium. The solution was extracted three times with CH_2Cl_2 (200 mL) and dried over Na_2SO_4. The combined organic extracts were concentrated *in vacuo*, and column chromatography [silica gel, Et_2O–light petroleum (60–80 °C) (1:1)] afforded 9,10-bis[(10-methyl-1,4,7,10-tetraoxadecyl)oxy]anthracene as a yellow solid (900 mg, 18%): ^1H NMR ($CDCl_3$, 200 MHz) δ 3.40 (6 H, s), 3.57–3.77 (8 H, m), 3.77 (8 H, s), 3.77–4.60 (8 H, m), 7.43–7.83 (4 H, m), 8.37–8.73 (4 H, m); IR (KBr) $\bar{\nu}_{max}$ 3020, 2940, 2900, 1680, 1620, 1480, 1460, 1440, 1410, 1380, 1360, 1340, 1310, 1290, 1270, 1250, 1200, 1180, 1150, 1110, 1070, 1030, 950, 930, 890, 860, 850, 810, 780, 650 cm^{-1}; MS (70 eV) *m/z* 502 (M^+, 7), 208 (20), 180 (17), 152 (11), 147 (21), 103 (23), 59 (100). Anal. Calcd for $C_{28}H_{38}O_8$: C, 66.91; H, 7.62; O, 25.46. Found: C, 66.75; H, 7.53; O, 25.37.

Photoproduct (Pd). UV irradiation (λ > 330 nm) of a degassed methanol (200 mL) solution of AAO_5O_5 (25 mg, 1.7×10^{-4} M) yields the photocyclomer (Pd) as the only photoproduct (20 mg; 80%): mp 142–145 °C; $\Phi_R \approx 4 \times 10^{-4}$; ^1H NMR ($CDCl_3$, 90 MHz) δ 3.90 (32 H, m, OCH_2CH_2O), 4.55 (2 H, m), 5.84 (2 H, m), 6.75 (2 H, m, β naphthalenic protons), 7.2–7.9 (10 H, m); IR (KBr) $\bar{\nu}_{max}$ 2925, 1460, 1100–1050, 800 cm^{-1}; UV λ_{max} (ϵ) (ethyl ether) 335 (1.1×10^3), 305 (3.2×10^3), 296 (4.3×10^3), 282 (5.5×10^3), 271 (7.6×10^3), 252 (3.0×10^3).

Photoproduct (Ps). UV irradiation (λ > 330 nm) of a degassed methanol (200 mL) solution of AAO_5O_5 (25 mg, 1.7×10^{-4} M) and $NaClO_4$ (37 g, 1.5 equiv) yields the photocyclomer (Ps), thermally unstable, which therefore was not isolated; evidence for the formation of the symmetrical 9,9′–10,10′ photoisomer (Ps) rests on the following observations: (i) the anthracenic band (310–420 nm) progressively disappeared with the corresponding growing up, not of the characteristic naphthalenic absorption band (335 nm), but rather of *o*-xylene units; (ii) in the dark, the photoproduct (Ps) underwent a nearly quantitative thermal back reaction (rate $k \approx 7 \times 10^{-4}$ s^{-1}) as observed for analogous bisanthracenes.[2a,16a,b]

Stability Constant Determination by Spectrophotometric Titration Procedures. The overall binding constants could be determined from the variations of either absorbance or fluorescence intensity at a fixed observation wavelength. In the case of a 1:2 stoichiometry, the overall binding constant, which controls the complexation equilibrium between the ligand L and the complex LM_2, is defined as the product of the stepwise binding constants K_{11} and K_{12} as follows, where L is the ligand and M the metal.

$$L + M \overset{K_{11}}{\rightleftharpoons} LM \qquad M + LM \overset{K_{12}}{\rightleftharpoons} LM_2 \tag{5}$$

$$K_{11} = \frac{[LM]}{[L][M]} \qquad K_{12} = \frac{[LM_2]}{[LM][M]} \qquad \beta = K_{11}K_{12} \tag{6}$$

The original method developed by Connors[20] has been derived to fit into our equations. At low concentrations, the optical response (absorption or emission) is directly proportional to the ligand concentration.

$$A_{sol} = k[L] \tag{7}$$

The mass balance equations for this overall process are

$$\begin{cases}[L]_{tot} = [L] + [LM] + [LM_2] \\ [M]_{tot} = [M] + [LM] + 2[LM_2]\end{cases} \quad (8)$$

When M is added to the solution, the optical response of the solution becomes

$$A_{sol} = a[L] + b[LM] + c[LM_2] + d[M] \quad (9)$$

If A_0 is the optical response of the free ligand in solution and A the optical response when no further changes occur upon addition of the metal M, eq 10 (where $\alpha = b - a - d$ and $\chi = c - a - 2d$) can be readily obtained provided a solution of the salt at the same concentration is placed in the reference beam.

$$\frac{A_{sol} - A_0}{A_{sol} - A_\infty} = K_{11}[M]_{tot}\frac{\alpha + K_{12}\chi[M]_{tot}}{(K_{11}[M]_{tot}(\alpha - \chi) - \chi)} \quad (10)$$

A computational fitting of the recorded experimental optical response with eq 10 allows the determination of the parameters α, χ, K_{11}, K_{12}, and consequently β. Using eq 10, satisfactory fits were obtained with Na^+ in either methanol or acetonitrile using both UV and fluorescence spectroscopies. With K^+ in methanol, K_{12} was found to be negligible ($<10^{-30}$) when the same equation is applied, indicating a 1:1 stoichiometry. As eq 5 is not well suited to this case, we established eq 11 (where $\gamma = (c - a - b)/a$) for the formation of a 1:1 weak complex.

$$\frac{A_{sol} - A_0}{A_0} = \gamma\frac{K_{11}[M]_{tot}}{1 + K_{11}[M]_{tot}} \quad (11)$$

Equation 7 gave good fits, therefore confirming a 1:1 stoichiometry for the K^+ complex.

A statistical calculation demonstrates that cooperativity arises when $K_{12}/K_{11} > 1/4$. Consider $\bar{\iota}$, defined as the average number of cations bound to one molecule of substrate (possessing two identical sites of complexation):

$$\bar{\iota} = \frac{[LM] + 2[LM_2]}{[M]_{tot}} \quad (12)$$

Using the equilibration constants it follows that

$$\bar{\iota} = \frac{K_{11} + 2K_{11}K_{12}[M]}{1 + K_{11}[M] + 2K_{11}K_{12}[M]^2} \quad (13)$$

This function can be readily developed using the MacLaurin formula ($c \in]0,[M][$)

$$\frac{\bar{\iota}}{[M]} = K_{11} + (2K_{11}K_{12} - K_{12}^2)[M] + \ldots + \frac{[M]^n}{n!}f^{(n)}(c) \quad (14)$$

when the slope of the tangent of the curve $\bar{\iota}/[M]$ at the abscissa 0 is positive, we can write

$$\frac{\partial(\bar{\iota}/[M])}{\partial[M]}|_0 > 0 \quad (15)$$

Deriving eq 10 gives

$$\frac{\partial(\bar{\iota}/[M])}{\partial[M]}|_0 \approx 2K_{11}K_{12} - K_{11}^2 > 0$$

and therefore $K_{12}/K_{11} > 1/2$.

Then, when the slope of the tangent of the curve $\bar{\iota}/[M]$ at the abscissa 0 is positive *a fortiori* $K_{12}/K_{11} > 1/4$ it is thus the evidence of a cooperative effect.

Acknowledgment. La région Aquitaine and the CNRS are thanked for partial financial support. The authors thank Prof. A. Castellan and Dr. M-H. Riffaud for initial work on this project and J.-C. Soulignac for valuable help with the Single Photon Timing equipment. We are indebted to Prof. F. De Schryver and Dr. N. Boens (Leuven Katholieke University) for providing the deconvolution program for the time dependent fluorescence intensity.

JO9513931